ELSEVIER

Chemical Engineering Journal 74 (1999) 181–196

Chemical Engineering Journal

Influence of the particle size distribution of powders on the velocities of minimum and complete fluidization

D. Gauthier*, S. Zerguerras, G. Flamant

Institut de Science et de Génie des Matériaux et Procédés, IMP-CNRS B.P. No. 5, Odeillo, F-66125 Font Romeu, France

Received 10 November 1998; received in revised form 23 February 1999; accepted 23 February 1999

Abstract

This paper presents the results of an experimental study dealing with the influence of the particle size distribution (PSD) on the fluidization regime. It was developed with Geldart B and D-type river sand. Five average diameters were considered between 282.5 and 1800 μm, and four PSD cases were studied for each of them: a reference (narrow cut) powder, a Gaussian-type powder, a binary mixture, and a flat (wide) PSD powder.

The Gaussian-type powders fluidize approximately at the same incipient fluidization velocities as the reference powders and therefore the minimum fluidization velocity of a Gaussian-type powder can be estimated by any correlation suitable for uniform-sized powders. On the contrary, flat PSD and binary mixtures have a very different hydrodynamic behavior, although similar to each other. For these mixtures, two characteristic velocities are needed to describe the behavior, i.e. the incipient and complete fluidization velocities.

Transition domains between incipient and complete fluidization were also investigated, and the experimental results show they depend to a large extent on the PSD: Gaussian mixtures hardly segregate and they behave like narrow range reference powders, whereas binary and flat PSD mixtures always segregate. It is shown that the transition domain extent is almost independent of the mixture mean diameter and nearly always between 30% and 45%. Experimental results for incipient fluidization and complete fluidization velocities are compared with the minimum fluidization velocity as predicted by several existing correlations for binary mixtures. Most of them are correct for average diameters smaller than 1.5 mm, but only one is satisfactory for larger diameters. Therefore we propose two *Re* versus *Ar* correlations for predicting the characteristic velocities that fit our experimental results obtained in a wide average diameter range.

It is found experimentally that the complete fluidization velocity is reduced with respect to the minimum fluidization of large particles when the average diameter increases for binary powders. The increasing influence of the small-to-big particles interaction for increasing average diameters may explain this finding. The results of calculations for the gas–particle and particle–particle interactions (i.e. collisions) in the case of the five considered binary powders show clearly that interparticle forces become significant ($\geqslant 5\%$) as soon as the average diameter is larger than 1 mm; this is in total agreement with our experimental results.

Keywords: Gas-solid fluidization; Particle size distribution; Particle-particle interaction; Minimum fluidization velocity; Complete fluidization velocity

1. Introduction

The particle size distribution (PSD) is known to have a strong influence on the hydrodynamics and related characteristics of gas–solid fluidized beds (such as mixing, conversion, etc. . .): in most cases, a narrow cut enhances the bed stability thus facilitating its operation (defluidizing, segregation and entrainment are reduced), although in some cases a wide PSD is found to be advantageous for ''fluidity'' and chemical conversion.

It is however of practical and economic interest to process wide PSD powders when dealing with ores and minerals or coal combustion: natural minerals are not extracted or commercialized with narrow PSDs because grinding and sieving are time and energy consuming duties, then using or valorizing only a fraction would be too costly. Moreover, in other applications such as drying, process engineers have to accept whatever PSDs are presented to them. It is therefore obviously worth studying how industrial processes behave in the case of wide PSD materials, since reducing grinding operations and replacing the sieves by a simple particle size classifier would save on investment and on operating cost. Moreover, the development of fluidized bed combustion/incineration processes (whether for solid fuels or for domestic and industrial solid wastes) stimulates the academic and industrial interests for treating wide size range powders.

*Corresponding author. Tel.: +33-04-68-30-77-57; fax: +33-04-68-30-29-40; e-mail: gauthier@imp-odeillo.fr

1385-8947/99/$ – see front matter
PII: S1385-8947(99)00075-3

The aim of this paper is to present the results of an experimental study dealing with the PSD influence on the onset of fluidization for Geldart B and D-type river sand. In order to do so, five powders with different mean diameters and four PSD cases for each of the powders were studied: a reference (narrow cut) powder, a Gaussian-type powder, a binary mixture, and a flat (wide) PSD powder. The ultimate objective of this study is to relate the PSD to the behavior of a given powder (like or unlike a simple and well-known narrow cut powder) and to predict the characteristic powder fluidization velocities.

2. Background

Early research in the late 1940's [1] concerning the influence of fines in powders was qualitative only and merely described the quality of mixtures and complete fluidization state. A few years later, Matheson et al. [2] studied the lubricating effect of fines added to catalyst powders, and this idea was later developed by others [3,4] who pointed out that the PSD has no influence either on the size of bubbles or on their frequency [5,6]. Sun and Grace [7] studied the influence of the PSD on the performances of catalytic fluid beds, and found out that purely including the fines content of a powder is not a sufficient parameter to characterize their effect: their nature and the overall size distribution have to be considered.

When fluidizing binary mixtures (whether particles have the same density such as considered in this study, or not), ''flotsam'' particles have the tendency to concentrate in the upper level of the bed, whereas ''jetsam'' particles accumulate in the lower part [8,9]; they will be referred hereafter by the subscripts ''f'' and ''j'', respectively. Two techniques are used for the experimental study of particle mixtures: one is based on the addition of fines in a powder initially composed of big particles only [1–8,10] thus leading to a variable mean diameter; the other is based on using the PSD mixture. We selected the latter technique which permits a better simulation of conditions encountered in industry. Several hydrodynamic studies [11–17] deal with the mixture segregation phenomena and three typical states can be obtained: perfect mixture, perfect segregation, and partial mixture of flotsam and jetsam particles. As a matter of fact, most papers dealing with mixture hydrodynamics concern the determination of characteristic velocities of powder layers with distributed size. Studies concern mainly binary and ternary mixtures [9,18–34], or even quaternary ones [35]. Studies are almost equally divided between homogeneous and heterogeneous mixtures since both of them are of concern for industrial applications. Often, wide PSD mixtures are considered as pseudo-binary ones [18,22,28]. These studies lead to several non-unanimously adopted characteristic velocities such as the apparent fluidization velocity (U_{fa}), the minimum fluidization velocity (U_{mf}), the complete fluidization velocity (U_{fc}), the initial fluidization velocity (U_{fi}), the segregation velocity (U_s),... which are determined by divers adaptations of the classical Richardson's method [36]. These velocities are mostly determined from ΔP versus U graphs for decreasing velocities. Some investigators [37–39] determine these velocities with increasing flowrates. Others [29,33–35] define the take-over velocity (U_{TO}), as the velocity where the physical forces promoting good mixing are equal to those promoting segregation; it corresponds to a mixing index M equal to 0.5 with M defined as the ratio of the mass fraction of jetsam in the uniform upper part of the bed and the average jetsam mass fraction in the fluid bed. Nienow et al. [35] indicate the strong influence of the distributor: they show that a perforated plate improves significantly mixing (less segregation tendency) compared to a porous plate.

Wide-range sized powders show fluidization characteristics very different from those of narrowly calibrated powders; particularly, the transition between fixed and complete fluidization states does not appear as a threshold but as a progressive phenomenon. Two unanimously adopted velocities can be identified, corresponding respectively to the incipient fluidization of the most fluidizable particles (U_{fi}) and to the complete fluidization of the whole set of particles in the mixture (U_{fc}); the wider the PSD, the wider the difference between these two velocities.

3. Experimental

3.1. Experimental set-up

The experimental set-up, designed to be operated at ambient conditions, is extensively described by Zerguerras [40]. The main element is a metacrylate transparent cylindrical column (internal diameter D_c=0.14 m; total height H_c=1.10 m). Air from a compressor is uniformly introduced into the column after flowing through a cone filled with metallic chips and a metallic plate composed of a 50 μm screen welded on a perforated plate grid (resulting distributor open area: 10%); at 0.5 m/s the pressure drop due to the whole distributor is 8.3 kPa. The actual gas flowrate is calculated from a rotameter reading and temperature and pressure corrections. The column is equipped with static pressure measurement probes located at the distributor level H_0=0, at H_1=0.015 m and at 12 other regularly set heights 0.025 m distanced from each other (H_2=0.040 m; H_3=0.065 m; H_5=0.090 m;...) to obtain either the differential pressure profile or the overall fluidized bed pressure drop. The temperature is measured at three locations in the bed by K-type thermocouples and averaged. Constant quantities of powder mixtures are introduced in the column for all the experiments, so as to give approximately the same fixed bed height of 0.28 m (=2D_c).

All data are transferred and recorded on a data acquisition set with variable acquisition frequency, and PC-treated.

3.2. Powders used

Powders of river sand of five mean diameters have been studied: d_1=282.5 μm; d_2=450 μm; d_3=900 μm; d_4=1425 μm; d_5=1800 μm. Powders d_1 and d_2 belong to Geldart's Group B [4], whereas the other three powders belong to Group D.

For each specific diameter, we considered:

1. A reference powder (R), defined as a narrow cut between two successive standard sieves; the average between both sieve openings determines the mean diameter.
2. A binary mixture (B), composed of two calibrated sets of particles, each about 50% in weight.
3. A Gaussian-type powder (G), prepared from five calibrated powders in proportions following a bell shape centered near the resulting mixture mean diameter; about 1/3 (in weight) of the particles have a diameter equal to the powder average diameter, whereas each of both extreme-sized particles proportions represents about 10% of the weight. So, the ratio standard deviation over average diameter σ/d_p of the resulting Gaussian is always equal to 0.34.
4. A flat (wide) PSD powder (F), which is prepared from five to six calibrated powders in almost equal proportions. The maximum gap between respective proportions is always less than 50%, and the biggest proportion is not necessarily the resulting average diameter; therefore these flat powders cannot be considered as flattened Gaussian mixtures.

In each case, all three mixtures have the same surface volume or Sauter mean diameter as the reference:

$$d_p = 1 \Big/ \left(\sum_i x_i / d_i \right), \quad (1)$$

with x_i the mass fraction of particles having d_i as average diameter.

All reference and mixed powders were prepared from natural river sand: they were obtained or reconstituted from as much as necessary narrow cuts between successive standard sieves, according to calculations to obtain a preset and required average diameter. The whole set of the 20 considered powder mixtures is described in Table 1. Fig. 1 illustrates the case of average diameter d_p=900 μm and the four PSD mixtures. For all other cases, the four PSD shapes are very similar.

3.3. Experimental procedure

The experimental procedure was selected after a set of preliminary experiments which were performed on binary mixtures, known to segregate thus expected to induce more experimental problems than other mixtures.

The total pressure drop variation versus gas velocity was studied with both increasing and decreasing gas velocities,

Table 1
Description of the considered powders and their PSDs

Type of powder	Weight % (x_i)	Sieves (mm)	Average diameter d_i (mm)
(A) *Composition for average diameter d_p=0.2825 mm*			
Reference	100	0.25–0.315	0.2825
Gaussian	9.0	0.16–0.2	0.18
	20.0	0.2–0.25	0.225
	34.0	0.25–0.315	0.2825
	24.0	0.315–0.4	0.3575
	13.0	0.4–0.5	0.45
Binary	45.0	0.2–0.25	0.225
	55.0	0.315–0.4	0.3575
Flat	17.0	0.16–0.2	0.18
	17.0	0.2–0.25	0.225
	19.0	0.25–0.315	0.2825
	23.0	0.315–0.4	0.3575
	24.0	0.4–0.5	0.45
(B) *Composition for average diameter d_p=0.45 mm*			
Reference	100	0.4–0.5	0.45
Gaussian	11.1	0.25–0.315	0.2825
	17.0	0.315–0.4	0.3575
	30.0	0.4–0.5	0.45
	23.0	0.5–0.6	0.55
	24.0	0.6–0.8	0.70
Binary	48.0	0.6–0.8	0.70
	52.0	0.25–0.4	0.325
Flat	13.8	0.25–0.315	0.2825
	16.7	0.315–0.4	0.3575
	16.7	0.4–0.5	0.45
	16.7	0.5–0.6	0.55
	16.7	0.6–0.8	0.70
	19.4	0.8–1.0	0.90
(C) *Composition for average diameter d_p=0.90 mm*			
Reference	100	0.8–1.0	0.9
Gaussian	10.0	0.5–0.6	0.55
	16.0	0.6–0.8	0.7
	36.0	0.8–1.0	0.9
	23.0	1.0–1.25	1.125
	15.0	1.25–1.6	1.425
Binary	56.0	0.6–0.8	0.7
	44.0	1.25–1.6	1.425
Flat	15.0	0.5–0.6	0.55
	17.0	0.6–0.8	0.7
	18.0	0.8–1.0	0.9
	23.0	1.0–1.25	1.125
	26.0	1.25–1.6	1.425
(D) *Composition for average diameter d_p=1.425 mm*			
Reference	100	1.25–1.6	1.425
Gaussian	10.0	0.8–1.0	0.9
	16.0	1.0–1.25	1.125
	37.0	1.25–1.6	1.425
	22.0	1.6–2.0	1.8
	15.0	2.0–2.5	2.25
Binary	45.0	1.0–1.25	1.125
	55.0	1.6–2.0	1.8
Flat	16.0	0.8–1.0	0.9
	16.0	1.0–1.25	1.125
	22.0	1.25–1.6	1.425
	23.0	1.6–2.0	1.8
	23.0	2.0–2.5	2.25

Table 1 (*Continued*)

Type of powder	Weight % (x_i)	Sieves (mm)	Average diameter d_i (mm)
(E) *Composition for average diameter d_p=1.8 mm*			
Reference	100	1.6–2.0	1.8
Gaussian	10.0	1.0–1.25	1.125
	16.0	1.25–1.6	1.425
	37.0	1.6–2.0	1.8
	23.0	2.0–2.5	2.25
	14.0	2.5–3.15	2.825
Binary	57.0	1.25–1.6	1.425
	43.0	2.5–3.15	2.825
Flat	16.0	1.0–1.25	1.125
	18.0	1.25–1.6	1.425
	18.0	1.6–2.0	1.8
	24.0	2.0–2.5	2.25
	24.0	2.5–3.15	2.825

and Fig. 2 illustrates a typical result (d_3=900 μm) expressed in relative values. Both profiles differ to a large extent, and since inertial phenomena have no significant effects in this case, the decreasing velocity profile is the only smooth one. Therefore, all the experiments to measure the characteristic fluidizing velocities (minimum, incipient and complete) were performed using the procedure with decreasing velocities.

In this preliminary phase, we also studied the influence of the initial state of the bed (well-mixed or partially-to-totally segregated) on the total pressure drop across the bed versus velocity plot. Fig. 3 illustrates the curve obtained with the binary mixture of average diameter d_3=900 μm. When starting from an initially segregated bed obtained from a mixed bed strongly fluidized and then segregated by reducing the velocity, the pressure drop is always less than in the case of a well-mixed initial mixture, and there exists no clear breakpoint in the profile. We also studied the influence of the initial bed state on the axial pressure drop profile within the bed itself (for a given gas velocity), using all the pressure probes along the column height. Observations differ from fixed to fluidized bed. In the fixed bed (see Fig. 4), the axial profile is linear when starting from a well-mixed state, like with a narrow range PSD reference powder. On the contrary, when starting from a segregated bed, there exists a breakpoint in the profile, and this point determines the limit accumulation height of the small particles, which appeared to be in good agreement with visual observation of the segregated layer through the transparent walls. This method is however very limited because it is almost impossible to

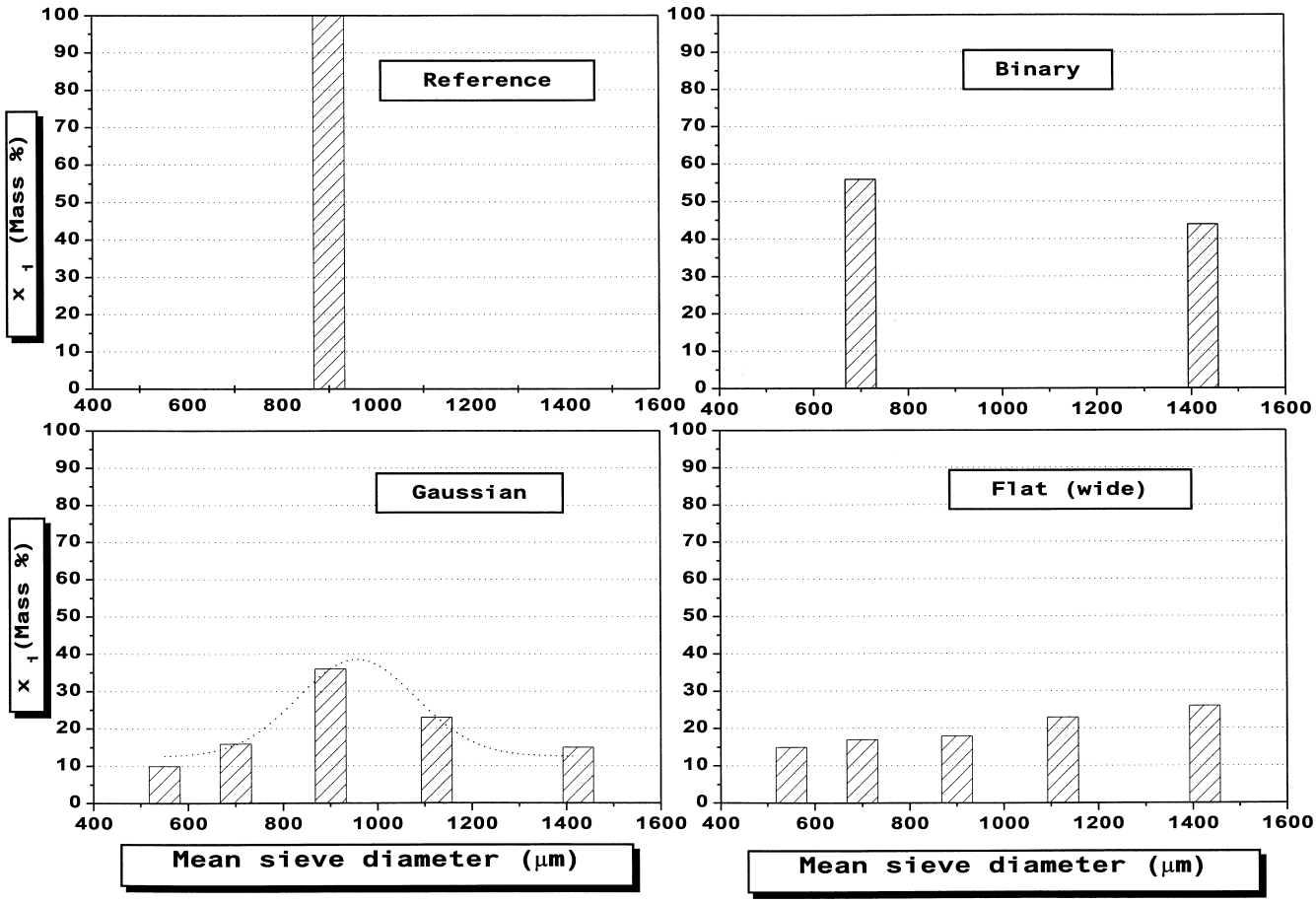

Fig. 1. PSD of the considered mixtures in the case d_p=0.900 mm.

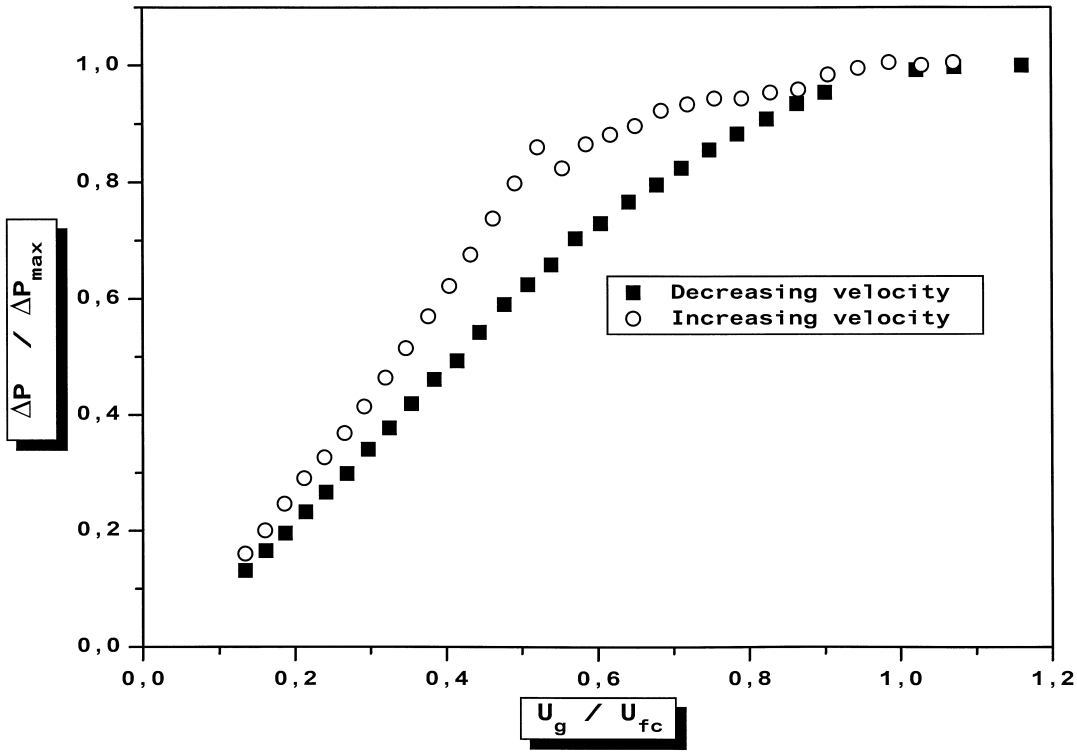

Fig. 2. Influence of the experimental procedure (increasing velocities–decreasing velocities) on the total pressure drop.

find a breakpoint in the curve for a semi-fluidized bed, although visually there is no doubt that segregation occurs. When the bed of a binary mixture is well-fluidized (very well-mixed), the axial pressure drop curve is linear as expected. This preliminary study showed therefore that it is impossible to use this kind of technique for a transient study of the segregation phenomena in the velocity range where it appears, since it is too difficult to estimate the

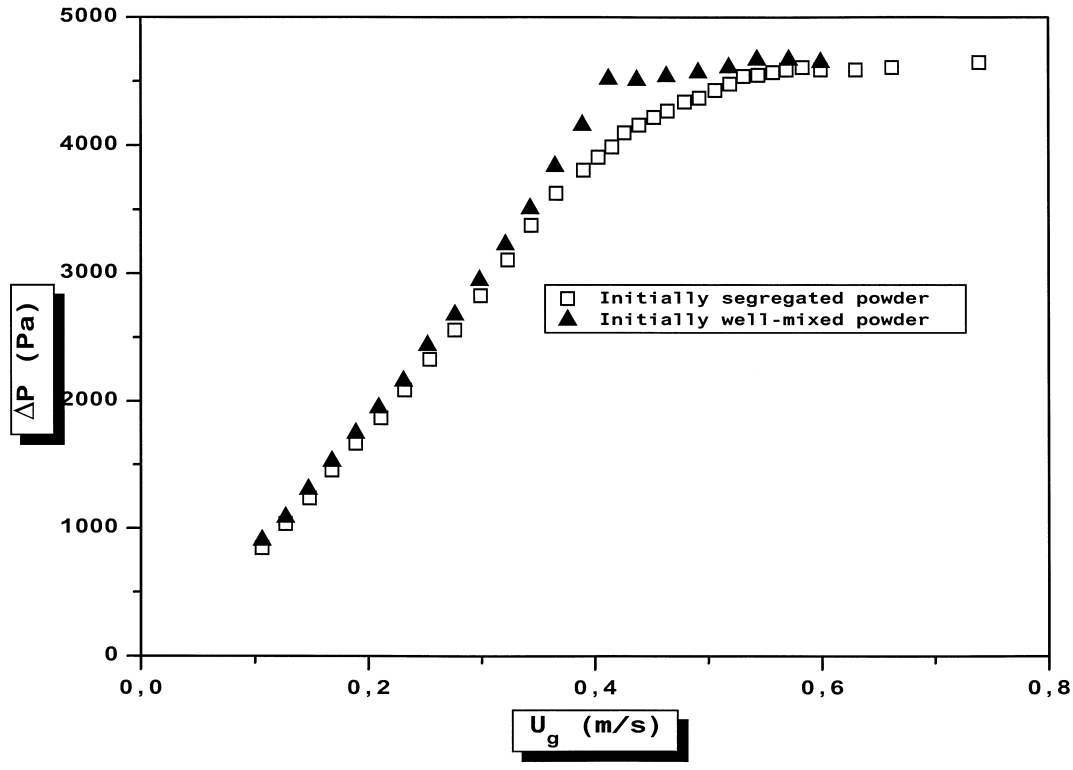

Fig. 3. Influence of the layer initial state on the total pressure drop.

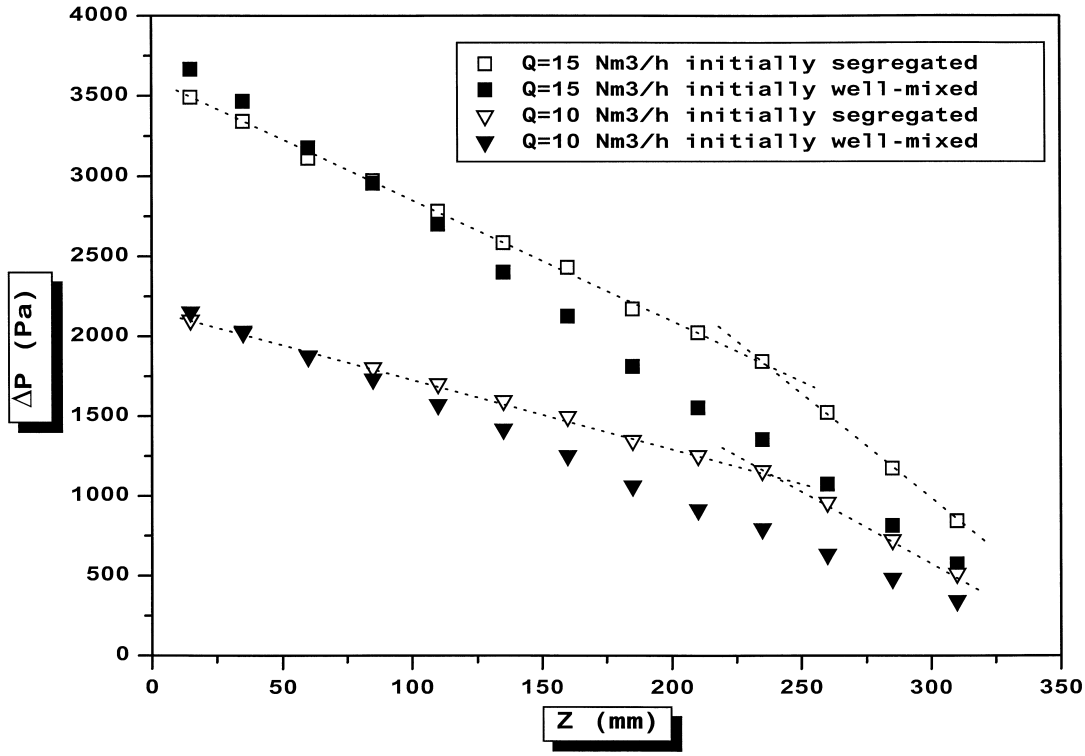

Fig. 4. Influence of the gas velocity on the axial pressure drop profile (binary mixture).

pressure drop profile breakpoint, especially for semi-fluidized bed.

It was therefore decided to use the well-known method recommended by Richardson [36]: the bed was first vigorously mixed by a high gas flowrate for half an hour, then the flowrate was gradually reduced and the total pressure drop due to the fluidized layer was recorded after 3–4 min in order to reach hydrodynamic equilibrium. Typical curves obtained are presented in Fig. 5. For reference powders, the minimum fluidizing velocity (U_{mf}) corresponds to the intersection between the horizontal plateau (well-fluidized bed) and the rising straight line (fixed bed). Characteristic velocities are different when dealing with mixtures where the limit between fixed and fluidized states is not defined by one single point, but two interesting velocities are important: the incipient

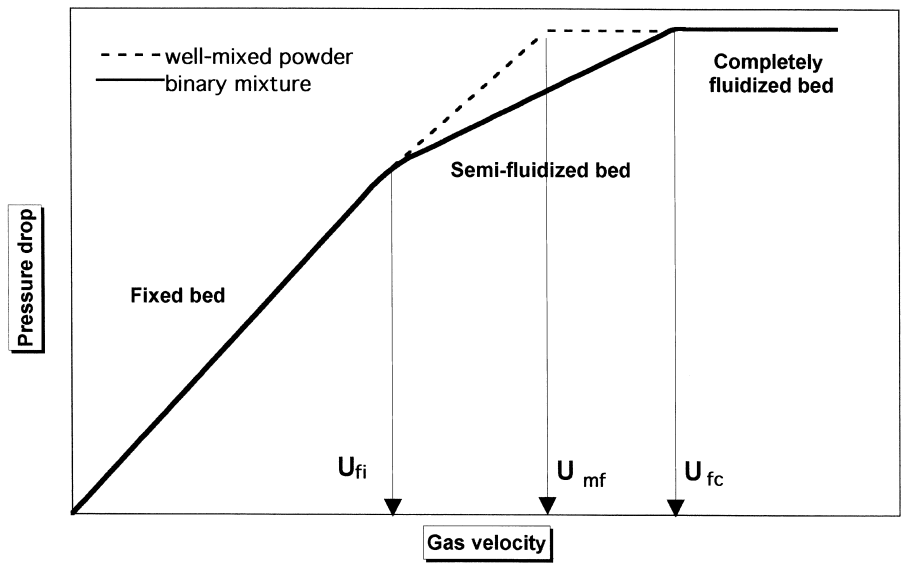

Fig. 5. Total pressure drop versus velocity profile, for both homogeneous powders and mixtures.

Table 2
Experimental minimum fluidization velocities of the reference powders

d_p (μm)	282.5	450	900	1425	1800
U_{mf} (m/s)	0.06	0.12	0.58	0.92	1.12
$E\ U_{mf}$ (%)	3.50	5.71	8.23	8.87	10.65
Re_{mf} (exp)	1.00	3.04	33.07	74.51	112.64
Ar	1866	7545	60 363	2.4×10^5	4.8×10^5

fluidization (U_{fi}) corresponding to the breakpoint in the ΔP versus U curve when the first particles begin to fluidize, and the complete fluidization (U_{fc}) when all particles are fluidized. The gas velocity domain between U_{fi} and U_{fc} will be called ''transition domain'' in this paper.

4. Experimental uncertainty

The considered mixtures have been prepared with 0.5% accuracy on the mass fractions and 2% accuracy on the average diameters, both imposed in the computer program used for calculating the different PSDs. The relative error on gas velocities varies between 2% in the fixed bed and 3% in the fluidized bed. For reference powders, the uncertainty on U_{mf} was experimentally defined by determining this velocity five to six times and calculating the average and deviation. The relative error on pressure drop measurements is function a of the fluidization state and thus on the gas velocity. When dealing with mixtures, it is small (2%) when the bed is fixed, since pressure fluctuations are low; it is around 7% when the bed is well-fluidized because of the bubble-induced strong pressure fluctuations; in the intermediate region corresponding to the semi-fluidized bed, we can assume it is the average (4.5%). The relative error induced by those on pressure drop measurements was then geometrically estimated from the plots as 9% for U_{fi} and 15% for U_{fc}. When appropriate, tables and plots presented hereafter include these calculated or estimated uncertainties.

5. Experimental results concerning the reference powders

Table 2 presents the influence of the particle diameter on the experimental minimum fluidizing velocity. It shows that the error on U_{mf} increases with the particle diameter (because of the increasing pressure fluctuations), ranging from 3.5% up to almost 11%. These results are also plotted in Fig. 6 which includes a set of experimental values from literature [37,41–44] obtained with narrow-sized particles having about the same density. The agreement is generally-speaking good to fair.

In addition, our experimental results concerning U_{mf} have been compared with the predictions of a selection of existing correlations whose parameters used for U_{mf} calculation are accessible. We define as the comparison criterion the relative difference on the Reynolds number at minimum fluidization according to

$$E\,Re_{mf}\,(\%) = 100 \times \left| \frac{Re_{mf}\,(\text{calc}) - Re_{mf}\,(\text{exp})}{Re_{mf}\,(\text{exp})} \right|. \qquad (2)$$

The list of the considered correlations drawn from literature [45–51] and the corresponding results are given in Table 3. Within the limits of their validity range, the correlations established by Wen and Yu [13], Bourgeois and Grenier [45], Thonglimp et al. [48,49], and Lucas et al. [50], which are similar since they were all obtained by modifying ERGUN's equation, are in best agreement with our results. Nevertheless, none of them give really satisfying results for diameter 450 μm, the error is nearly always bigger than 50%.

Table 3
Comparison of experimental results concerning U_{mf} with the predictions from several existing correlations

Authors	Correlation	$E\ Re_{mf}(\%)=f(d_p\ (\mu m))$				
		282.5	450	900	1425	1800
Wen and Yu [13]	$Re_{mf}=(33.7^2+0.0408\ Ar)^{0.5}-33.7$	11.1	41.1	20.5	5.6	1.7
Bourgeois and grenier [45]	$Re_{mf}=(25.46^2+0.0382\ Ar)^{0.5}-25.46$	–	–	12.7	1.3	0.0
Saxene and Vogel [46]	$Re_{mf}=(25.28^2+0.057\ Ar)^{0.5}-25.28$	102.2	143	16.7	26.5	26.5
Richardson and St. Jeronimo [47]	$Re_{mf}=(25.7^2+0.0365\ Ar)^{0.5}-25.7$	29.3	60.9	15.9	30.1	2.7
Thonglimp et al. [48,49]	$Re_{mf}=7.54\times10^{-4}\ Ar^{0.98}$ Re<30	21.0	56.5	–	–	–
	$Re_{mf}=1.95\times10^{-2}\ Ar^{0.66}$ 30<Re<180	–	–	–	7.1	2.2
	$Re_{mf}=(31.6^2+0.0425\ Ar)^{0.5}-31.6$	23.1	55.2	15.0	0.0	2.1
Lucas et al. [50]	$Re_{mf}=(29.5^2+0.0357\ Ar)^{0.5}-29.5$	10.8	40.1	22.9	9.2	7.1
Tannous [26]	$Re_{mf}=0.03\ Ar^{0.63}$	244	173	6.8	1.4	1.5
	$Re_{mf}=(25.83^2+0.043\ Ar)^{0.5}-25.83$	50.9	86.1	5.4	5.9	7.0
Barbosa et al. [51]	$Re_{mf}=1.9\times10^{-3}\ Ar^{0.87}$	33.2	47.7	17.3	22.3	47.8

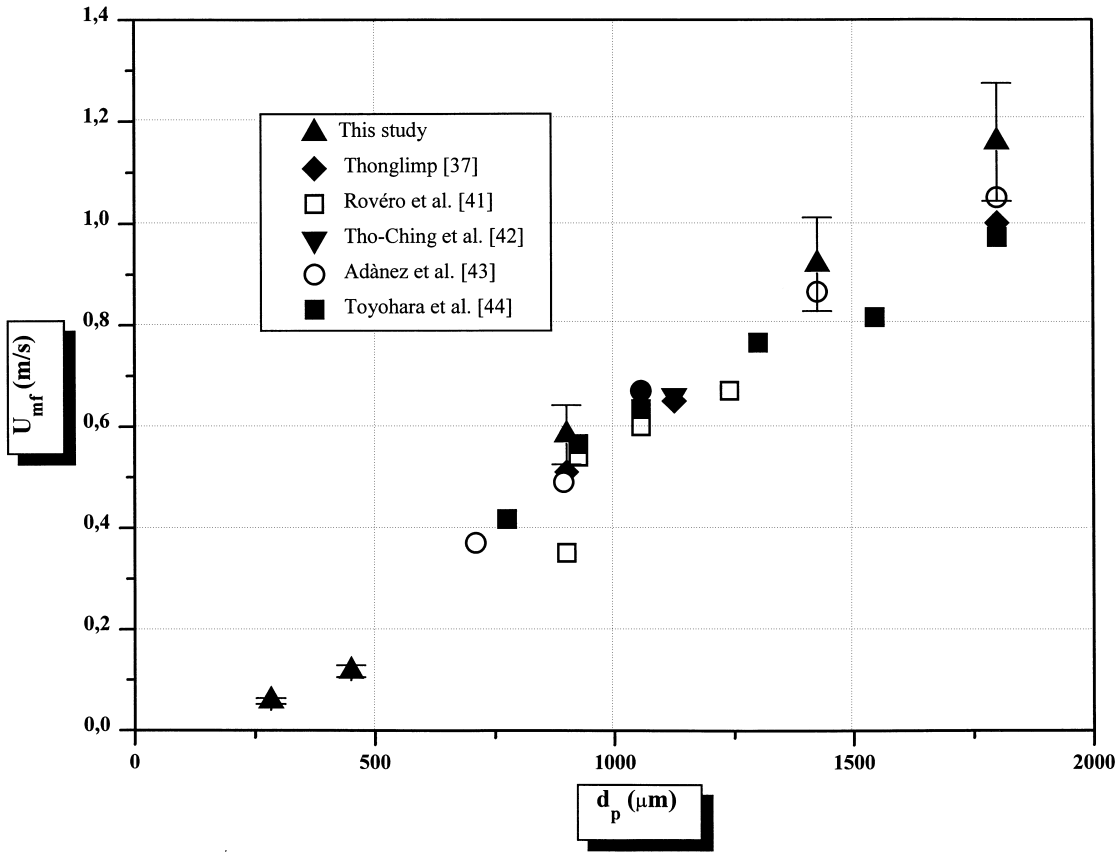

Fig. 6. Influence of the powder average diameter on the U_{mf} (reference powders).

6. Experimental results concerning the size-distributed powders

The hydrodynamic behavior of the different powders is illustrated by determining the characteristic velocities from plotting the total pressure drop across the fluidized bed versus gas velocity.

6.1. Behavior of Gaussian-type powders

As shown in Fig. 7, the Gaussian-type powders have a hydrodynamic behavior similar to that of the corresponding reference powders with clearly defined fixed bed and fluidized bed regions: U_{mf} is readily defined.

Fig. 8 compares the minimum velocities for both Gaussian and reference powders for the five considered mean diameters: the Gaussian-type powders fluidize almost exactly at the same velocities as the reference powders and the influence of small proportions of extreme-sized particles is insignificant (particles remain well-mixed when defluidizing the bed). Within the studied interval (282.5–1800 μm), a Gaussian-type powder characteristic velocity can be estimated from any good correlation proposed for uniform-sized powders.

6.2. Behavior of binary and flat PSD powders

When defluidizing a binary mixture, segregation occurs and leads to the concentration of big particles at the lower part of the bed while small ones concentrate at the upper part. These two zones are separated by a third intermediate one, composed of the mixture small–big, whose thickness decreases with the gas velocity to the advantage of both preceding zones.

Flat PSD and binary mixtures have a similar hydrodynamic behavior, although very different from that of reference powders. As shown in Figs. 9 and 10, the total pressure drop versus gas velocity profile presents two breakpoints corresponding to incipient fluidization (U_{fi}) and complete fluidization (U_{fc}) velocities.

6.3. Influence of the average diameter on U_{fi} and U_{fc}

The influence of the powder diameter on the characteristic velocities is given in Table 4 and plotted in Fig. 11, which contains for comparison U_{mf} values for reference powders. Both U_{fi} and U_{fc} variations with mixture average diameter are S-shaped, which is very different from the almost straight reference line. The curves tend to flatten

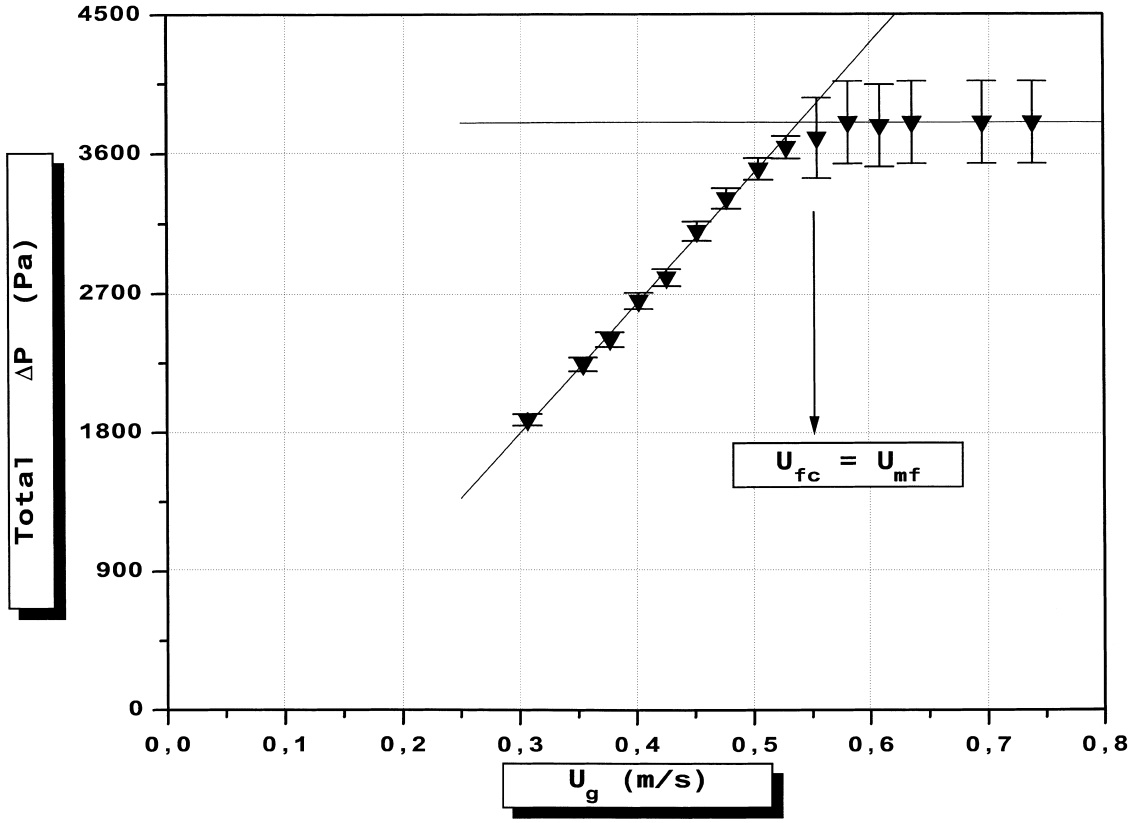

Fig. 7. Total pressure drop versus velocity profile in the case of a Gaussian powder (d_p=0.900 mm).

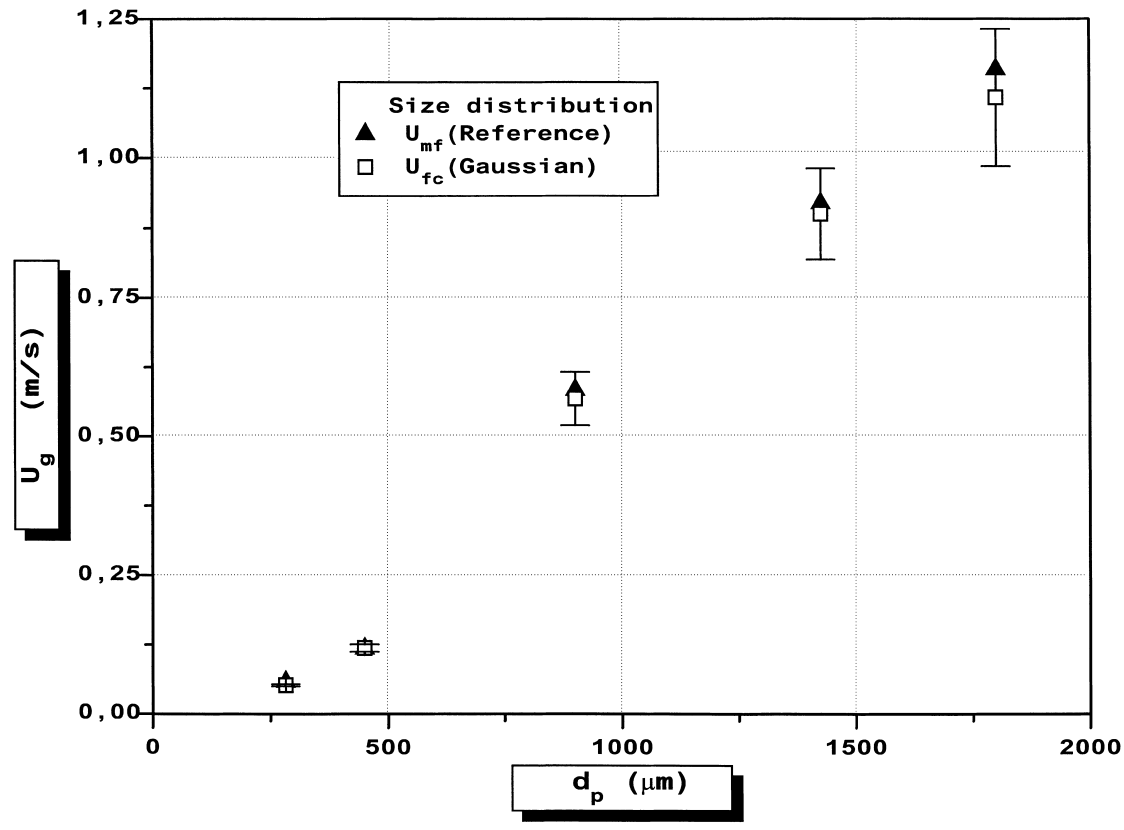

Fig. 8. Influence of the powder d_p on the U_{mf} comparison between reference and Gaussian powders).

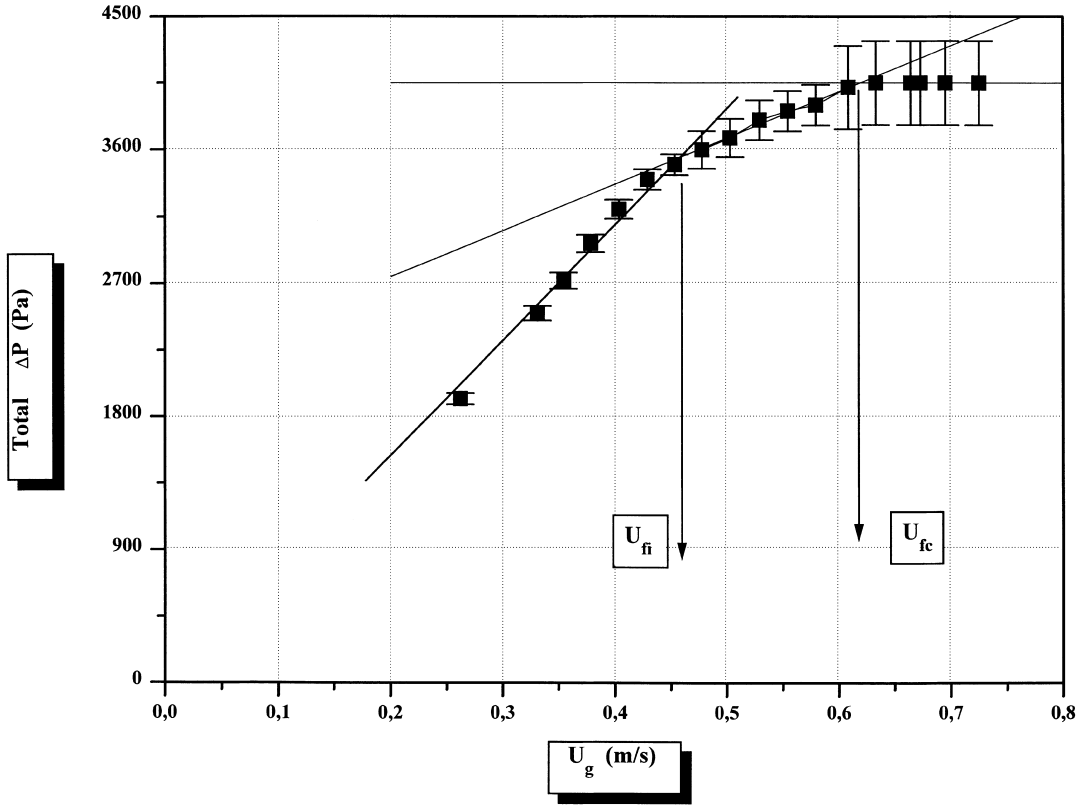

Fig. 9. Total pressure drop versus velocity profile in the case of a Binary powder d_p=0.900 mm).

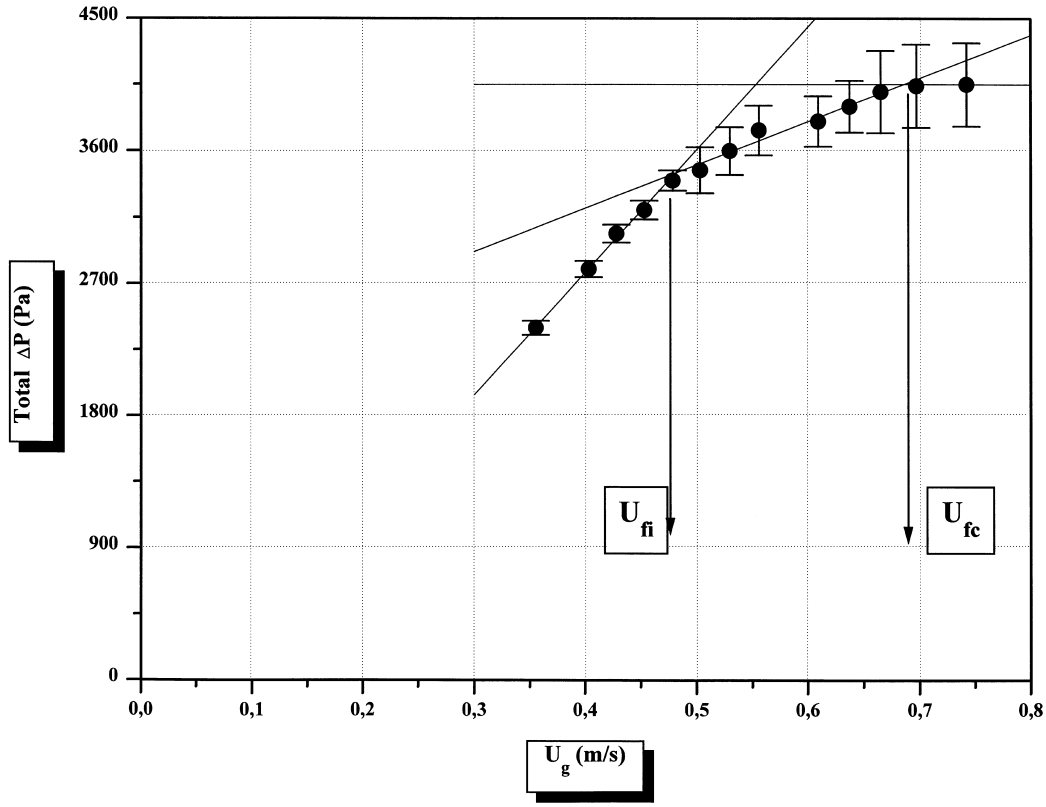

Fig. 10. Total pressure drop versus velocity profile in the case of a flat powder d_p=0.900 mm).

Table 4
Experimental characteristic velocities of the considered powders

PSD	Velocity (m/s)	Powder averate diameter (μm)				
		282.5	450	900	1425	1800
Reference	U_{mf}	0.06	0.12	0.58	0.92	1.12
Gaussian	$U_{fc} \approx U_{mf}$	0.05	0.12	0.57	0.90	1.11
Binary	U_{fi}	0.04	0.12	0.44	0.73	0.80
	U_{fc}	0.08	0.17	0.62	1.08	1.16
Flat	U_{fi}	0.05	0.12	0.48	0.71	0.74
	U_{fc}	0.08	0.18	0.69	0.98	1.08

when increasing the average diameter while U_{mf} increases constantly, thus showing that the difference in behavior increases with the diameter.

6.4. Influence of the PSD on the transition domain extent

The segregation phenomenon depends largely on the PSD: Gaussian mixtures, in which the major fraction is that of the reference powder, hardly segregate and they behave like the reference powders, probably because extreme-sized particles are present in small quantities only. On the contrary, binary and flat PSD mixtures always segregate. In order to quantify the extent of the segregation and its evolution with the average diameter, the relative difference between both incipient fluidization and complete fluidization velocities is considered and illustrated in Fig. 12.

$$\mathrm{ES}(\%) = 100(U_{fc} - U_{fi})/U_{fi}. \quad (3)$$

The relative difference, thus the extent of the segregation range, is almost independent of the mixture average diameter and is approximately 30%, except for the smallest studied average diameter (282.5 μm) for which it is about 45%.

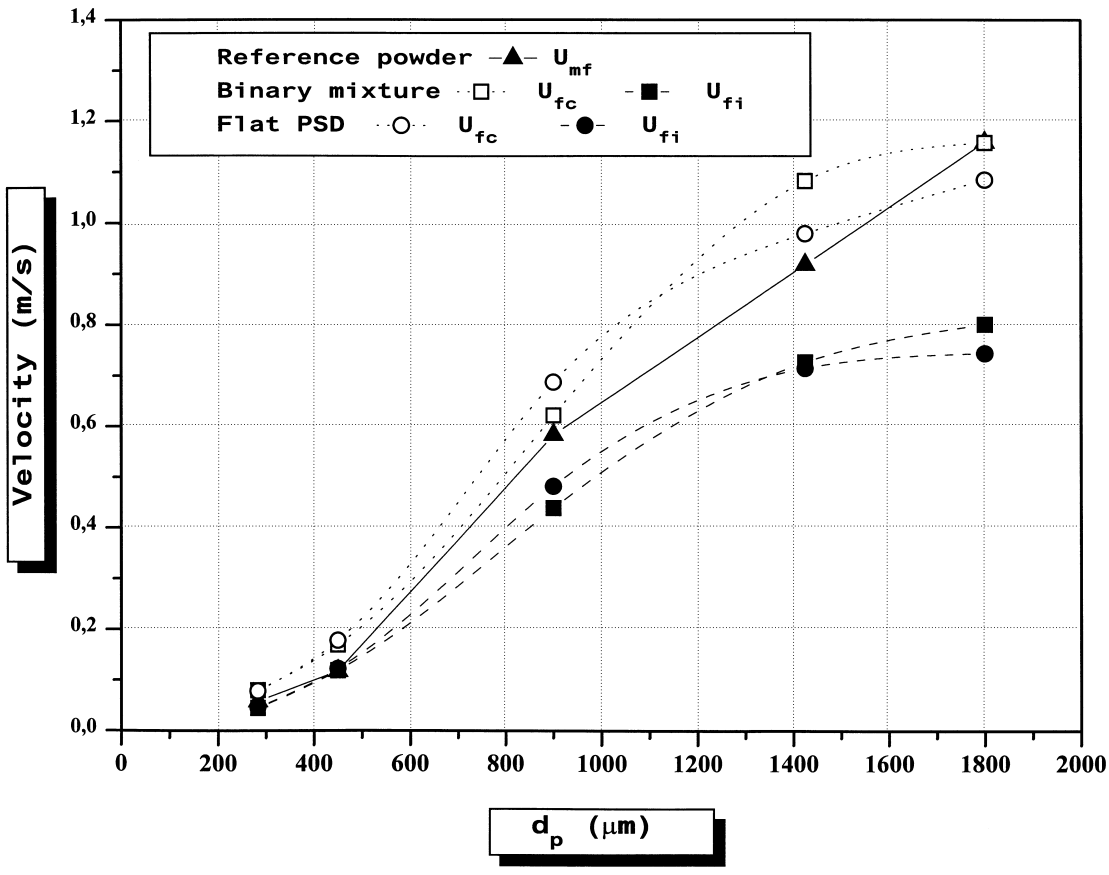

Fig. 11. Influence of the powder d_p on the fluidization characteristic velocities (comparison between reference powders and both flat and binary mixtures).

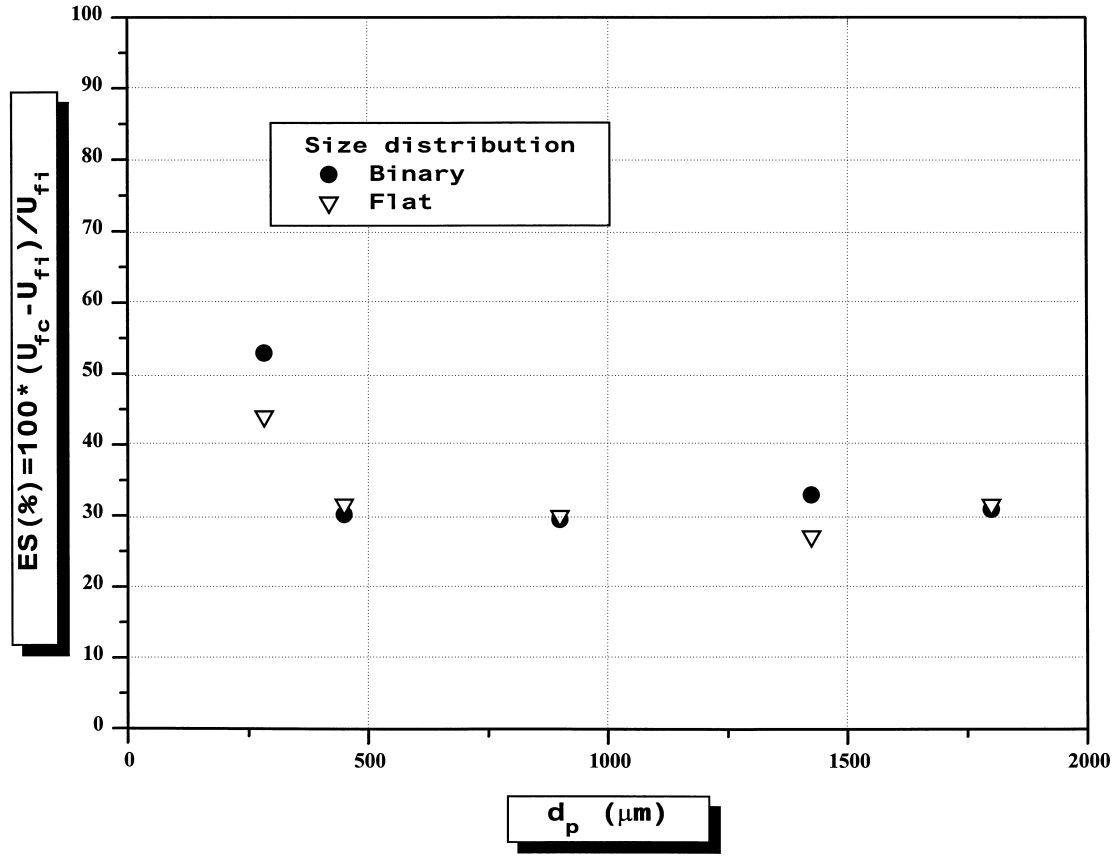

Fig. 12. Influence of the powder d_p on the relative difference between U_{fi} and U_{fc} (flat and binary mixtures).

7. Correlations for predicting the segregating mixtures characteristic velocities

Our experimental results are plotted in Fig. 13, together with results from other studies [12,26] and with U_{mf} predictions from existing correlations [9,13,19,32]. As can be seen, all considered correlations but one [32] are rather satisfying for small average diameters (up to 1500 μm) since they predict correctly U_{mf} between U_{fi} and U_{fc}. But Wen and Yu's correlation [13] (which is in fact a compilation of correlations) is the only one still correct for bigger average diameters. This may be the result of the fact that these correlations were established with heterogeneous mixtures [19,32] or for narrow diameter range [9]. The results can be expressed by using the classical dimensionless numbers when dealing with hydrodynamics, i.e. the Reynolds and Archimedes numbers. Fig. 14 plots *Re* versus *Ar* for incipient fluidization and complete fluidization in the case of homogeneous segregating mixtures. Binary and flat PSD mixtures having a similar behavior, the considered velocities are average values. Our whole set of experimental results can be very satisfactorily fitted by

$$Re_{fi} = 2.2 \times 10^{-3}\ Ar^{0.818} \text{ in the range } 0.78 < Re_{fi} < 78 \text{ and } 1800 < Ar < 5 \times 10^5, \quad (4)$$

$$Re_{fc} = 5.2 \times 10^{-3}\ Ar^{0.777} \text{in the range } 1.35 < Re_{fc} < 113 \text{ and } 1800 < Ar < 5 \times 10^5$$

with the correlation coefficients 0.998 and 0.994 for incipient and complete fluidization, respectively. Notice that these correlations have been established with homogeneous mixtures, fluidized in deep beds with a perforated plate distributor, and their validity should be checked before using them in other conditions. However, since they have to do only with physical quantities, they are more convenient than other correlations introducing parameters such as, for example, the bubble diameter [34] which can be determined only in transparent-wall vessels or have to be estimated from known correlations.

8. Interpretation of the results

The effect of fine particles on the onset of fluidization of large particles has been widely studied but almost only in the case of binary mixtures, and in most studies mixtures are considered as the equivalent bed with a single Sauter average diameter. Our experimental results show that the U_{fc} versus d_p curve has the characteristic shape, as shown in Fig. 11. This trend shows the decrease of the difference

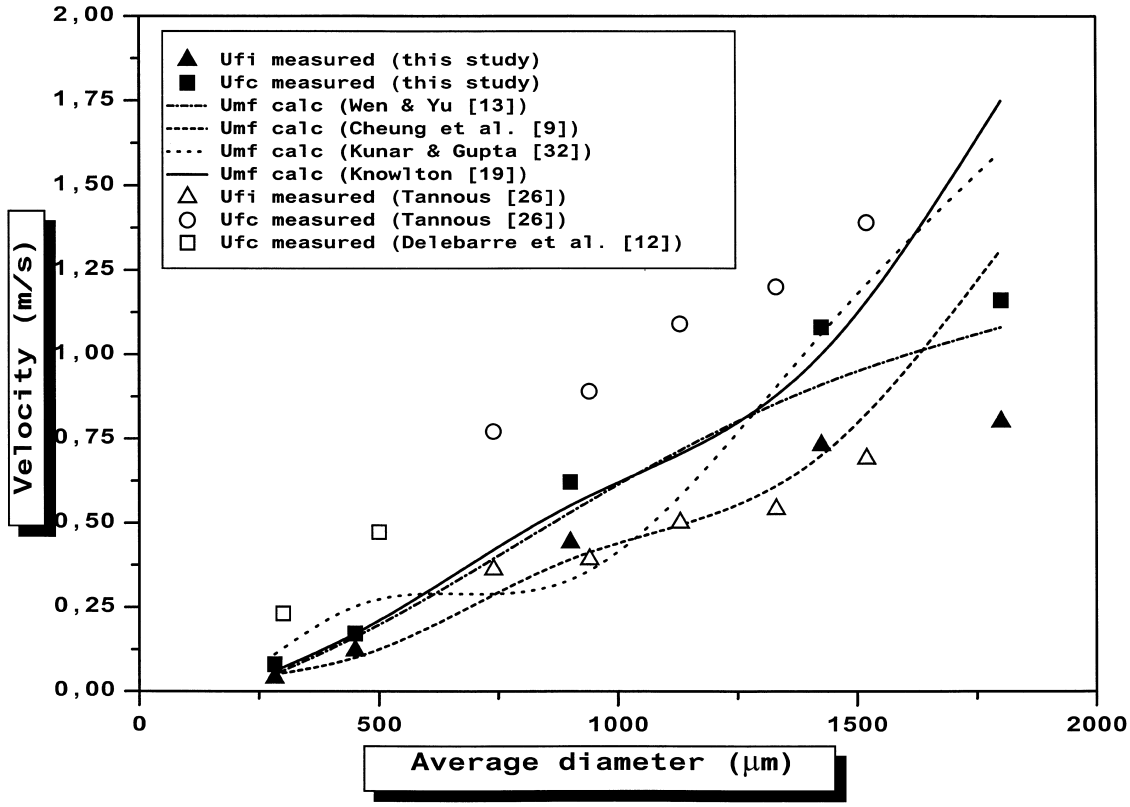

Fig. 13. Segregating mixtures characteristic velocities: comparison between experimental results and results from literature.

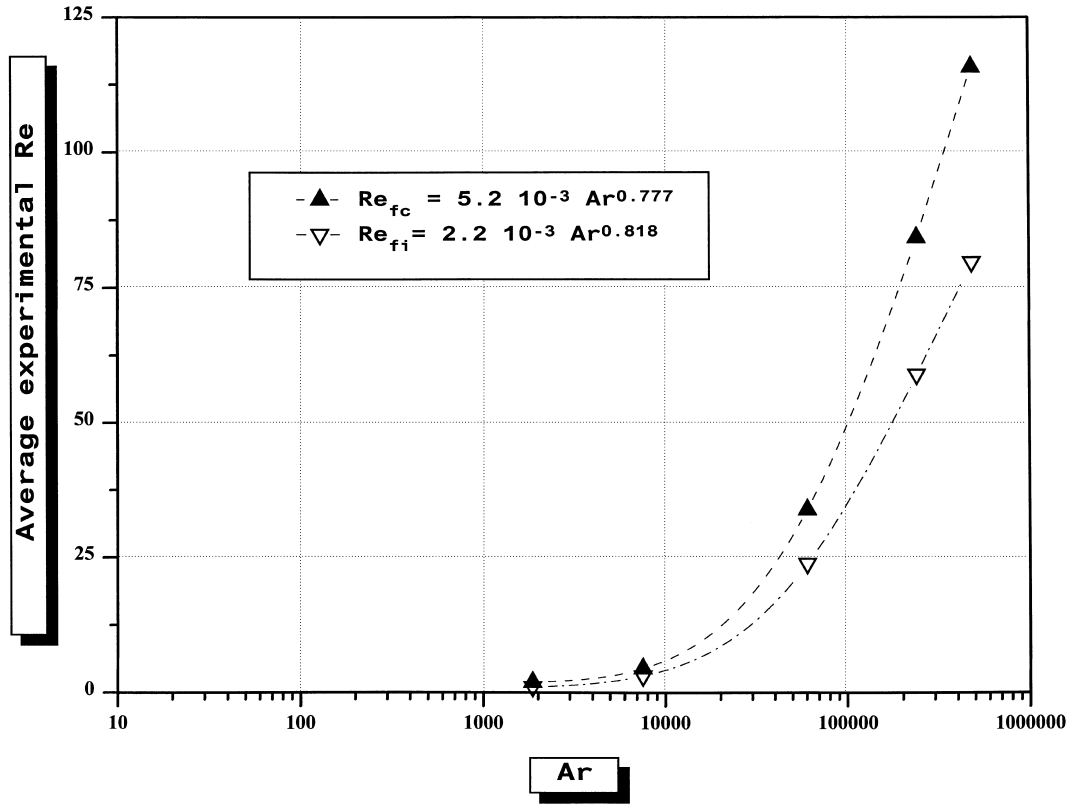

Fig. 14. *Re* versus *Ar* at incipient fluidization (Re_{fi}) and at complete fluidization (Re_{fc}).

$U_{fc}-U_{mf}$ with the average particle diameter (it becomes null for d_p=1.8 mm), which may be analyzed as an increase of the fine-to-large particle collision contribution. For gas velocities ranging between U_{fi} and U_{fc}, one may consider that small particles are fluidized whereas big ones are still fixed: the forces acting vertically on the small particles and inducing their movements are, in addition to the weight, due to gas–particle interaction and particle–particle interaction, i.e. collisions. The effect of fine particles in a bed of large ones has been recently studied by Talukdar and Mathur [52], who used Marble's [53] one-dimensional approach for particle collisions, considering perfectly elastic collisions between small and large spherical bodies.

Let consider a mixture of large (d_j) and small (d_f) particles of the same material and equal density, flowing in a gas with respective velocities U_j, U_f and U_g in the z direction (1-D approach). If $F_{pp}(d_j,d_f)$ is the force per unit volume exerted upon particles of diameter d_j by particles of diameter d_f and $F_{gp}(d_j)$ is the viscous force per unit volume due to the gas–particle interaction, forces can be expressed according to Marble [53] as follows:

$$\frac{F_{pp}(d_j,d_f)}{F_{gp}(d_j)}=\left(\frac{\tau_v(d_j)}{\tau_c(d_j)}\right)\left(\frac{d_f^3}{(d_j^3+d_f^3)}\right)\left[\frac{(U_f-U_j)}{(U_g-U_j)}\right] \quad (5)$$

with

$$\frac{\tau_v(d_j)}{\tau_c(d_j)}=\left(\frac{1}{12}\right)\left[\frac{(d_j+d_f)|U_j-U_f|}{v_g}\right]\left(\frac{\rho_f}{\rho_g}\right)\left[\frac{(d_j+d_f)\cdot d_j^2}{d_f^3}\right]. \quad (6)$$

The first term in brackets in Eq. (6) is similar to a Reynolds number. The relation in Eq. (6) is the ratio of two characteristic times related to viscous and collision interactions; the validity of this expression is restricted to $\tau_v/\tau_c\{\leqslant\}1$. τ_v is the time required for the particle slip velocity to decay to $1/e$ of its initial value, and τ_c is the time duration between two collisions.

Considering the respective values of the velocities at the threshold value (U_{fc}), it is assumed:

$$U_j=0, U_g=U_{fc}/\varepsilon,\ U_f\rightarrow U_g.$$

This model is applied for gas velocity U_g given by U_{fc}/ε at complete fluidization and considering that the big particles are fixed, U_j=0, and that the maximum velocity of fine particles is that of the gas $U_g(max)=U_{fc}/\varepsilon$. As a consequence, the calculation gives the maximum value of the F_{pp}/F_{gp} ratio when the fluidization superficial velocity is U_{fc}.

The results of the calculations in the case of the considered binary powders are given in both Table 5 and Fig. 15, which plots the ratio $F_{pp}(d_j,d_f)/F_{gp}(d_j)$ versus d_p.

Table 5
Ratio F_{pp}/F_{gp} as a function of d_p for the considered binary powders

d_p (μm)	282.5	450	900	1425	1800
F_{pp}/F_{gp} (%)	0.002	0.6	4.7	11.0	(17.7)

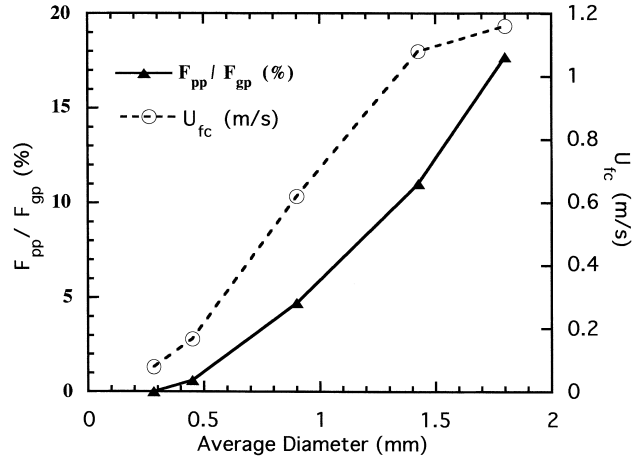

Fig. 15. Influence of the powder d_p on the ratio F_{pp}/F_{gp}.

Fig. 15 shows clearly that particle–particle collision forces play a more and more significant role when d_p increases, and they become significant ($\geqslant$5%) as soon as the mean diameter is larger than 1 mm. This is in agreement with our experimental results (see Fig. 11). The ratio of collision versus viscous forces reaches 11% for d_p=1.425 mm. The result for d_p=1.8 mm is only indicative since in this case τ_v/τ_c=1.5, and therefore the approximation is no longer valid.

9. Conclusion

In this paper, the results of an experimental study dealing with the PSD influence on the onset of fluidization are presented. This study was developed with B- and D-type river sand-based powders, according to Geldart's classification; five average diameters were considered in the range 282.5–1800 μm, and for each of them, four PSD were studied: a reference (narrow cut) powder, a Gaussian-type PSD powder, a binary mixture, and a flat and wide PSD powder.

A preliminary study showed that when segregation appears, it is impossible to follow its front progress from the axial pressure drop profile in the bed transient evolution (for a given gas velocity), since it is impossible to estimate the pressure drop profile break-point in the semi-fluidized zone.

The Gaussian-type PSD powders fluidize almost exactly at the same velocities as the reference powders thus showing that the influence of extreme-sized particles in small proportions is insignificant. So, a Gaussian-type PSD powder characteristic velocity (minimum fluidization velocity) can be estimated from any good classical correlation proposed for uniform-sized powders. On the contrary, flat PSD and binary mixtures have very different hydrodynamic behaviors, although similar to each other. In these two cases, the total pressure drop versus gas velocity profile presents two

break-points corresponding to incipient fluidization and complete fluidization velocities.

The transition phenomenon depends strongly on the PSD: Gaussian mixtures do hardly segregate and they behave just like narrow range reference powders, whereas binary and flat PSD mixtures always segregate, which comes from extreme-sized particles which are not present in small proportions. The relative difference between both incipient fluidization and complete fluidization velocities, that-is-to-say the transition domain extent, is almost independent of the (homogenous) mixture average diameter; it is always 30%, except for the smallest studied mean diameter (282.5 μm) for which it is about 45%. Several existing correlations were considered and tested for fitting our experimental results. A satisfying fit could hardly be obtained for average diameter bigger than 1500 μm. This is the reason why we propose two correlations based on our results for predicting incipient and complete fluidization velocities.

$$Re_{fi} = 2.2 \times 10^{-3}\ Ar^{0.818} \text{ with } 0.78 < Re_{fi} < 78 \text{ and } 1800 < Ar < 5 \times 10^5,$$

$$Re_{fc} = 5.2 \times 10^{-3}\ Ar^{0.777} \text{ with } 1.35 < Re_{fc} < 113 \text{ and } 1800 < Ar < 5 \times 10^5$$

Our experimental results show for binary powders that the U_{fc} versus d_p curve has a characteristic shape which seems to prove an increasing influence of the particles interaction with the average diameter: the complete fluidization velocity U_{fc} is reduced with respect to the minimum fluidization of large particles. The results of calculations, taking into account the gas–particle interaction and particle–particle interaction, i.e. collisions, show clearly in the case of the considered binary powders that inter-particle forces play a more and more significant role when d_p increases, and they become significant ($\geqslant 5\%$) as soon as the average diameter is bigger than 1 mm. This point is in total agreement with our experimental results.

10. Nomenclature

D_c	column inside diameter (m)
$d_1, d_2, \ldots, d_5, d_i$	considered mixtures mean diameter (m)
d_p	powder harmonic average diameter (surface-volume diameter) (m)
ES(%)	relative difference between incipient fluidization and complete fluidization velocities
F	force (N)
F_{gp}	viscous force per unit volume due to gas–particle interaction (N/m^3)
F_{pp}	force per unit volume due to particle–particle interaction (N/m^3)
H_c	column total height (m)
M	mixing index
M	single particle mass (kg)
P	pressure (Pa)
ΔP	pressure drop (Pa)
U	gas velocity (m/s)
x_i	mass fraction of particles with mean diameter d_i
Z	distance from the grid (m)
ε	bed porosity
μ	dynamic viscosity (Pa·s)
v	kinematic viscosity (m^2/s)
ρ	density (kg/m^3)
σ	standard deviation
τ_c	$\tau_c = 1/N_c$ (s) where N_c is the collision frequency
τ_v	$\tau_v = m/6\pi d\mu$ (s)

Dimensionless numbers

Ar	Archimedes number $= d_p^3 \rho_g (\rho_s - \rho_g) g/\mu_g^2$
Re	Reynolds number $= d_p U \rho_g / \mu_g$

Subscripts

B	binary mixture
c	collision
f	flotsam particles
fa	apparent fluidization
fc	complete fluidization
fi	initial fluidization
F	flat and wide PSD mixture
g	gas
G	Gaussian-type PSD mixture
j	jetsam particles
mf	minimum fluidization
p	particle
R	reference powder
s	segregation
TO	take-over
v	viscous

References

[1] J.D. Parent, N. Yagol, C.S. Steiner, Chem. Eng. Prog. 43 (1947) 429.
[2] G.L. Matheson, W.A. Herbst, P.H. Holt, Ind. Eng. Chem. 41 (1949) 1109.
[3] F.A. Zenz, D.F. Othmer, Fluidization and Fluid-particle Systems, Reinhold, New York, 1960.
[4] D. Geldart, Powder Technol. 7 (1973) 285–292.
[5] R.J. Clift, J.R. Grace, Trans. Ins. Chem. Eng. 50 (1972) 364.
[6] G. Sun, J.R. Grace, AIChE J. 38(5) (1992) 716–722.
[7] G. Sun, J.R. Grace, Chem. Eng. Sci. 45 (1990) 2187–2195.
[8] P.N. Rowe, A.W. Nienow, A.J. Agbim, Trans. Ins. Chem. Eng. 50(1) (1972) 310–323.

[9] L. Cheung, A.W. Nienow, P.N. Rowe, Chem. Eng. Sci. 29 (1974) 1301–1303.
[10] B. Formisani, Powder Technol. 66 (1991) 259–264.
[11] A.B. Delebarre, Powder Technol. 75 (1993) 181–187.
[12] A.B. Delebarre, A. Pavinato, J.C. Leroy, Powder Technol. 80 (1994) 227–233.
[13] C.Y. Wen, Y.H. Yu, Chem. Eng. Prog. Symp. Series 62 (1966) 110–111.
[14] P.T. Shannon, Ph.D. Thesis, Illinois Inst. Technol., Chicago, USA, 1961, quoted by Tannous [26].
[15] J. Bena, I. Hadalde, M. Bafrnec, J. Ilavsky, Coll. Czechoslov. Chem. 33 (1968) 2620 quoted by TANNOUS [26].
[16] K. Noda, S. Ushida, T. Makino, H. Kamo, Powder Technol. 46 (1986) 149–154.
[17] G. Kwant, W. Prins, W.P.M. Van Swaaij, Powder Technol. 82 (1995) 279–291.
[18] J.L. Chen, D.L. Keairns, Can. J. Chem. Eng. 53 (1975) 395–401.
[19] T. Knowlton, AIChE Symp. Ser. 161(73) (1977) 22–27.
[20] S. Chiba, T. Chiba, A.W. Nienow, Kobayashi, Powder Technol. 22 (1979) 255–269.
[21] A. Lucas, J. Arnaldos, J. Casal, L. Puigjaner, Chem. Eng. Comm. 41 (1986) 121–132.
[22] S. Cobbinah, C. Laguerie, M. Avaro, T. Baron, Symp. Séparation, Mélange, Réactions, Etudes finalisées, Groupe Français de Génie des Procédés Toulouse, Lavoisier Technique et Documentation, Paris, 1989, pp. 131–136.
[23] B. Taha, Thèse de doctorat, Université des Sciences et Techniques de Lille-Flandres-Artois, Lille, France, 1989.
[24] G.K. Khoe, T.L. Ip, J.R. Grace, Powder Technol. 66 (1991) 127–141.
[25] G. Sun, J.R. Grace, AIChE J. 38(5) (1992) 716–722.
[26] K. Tannous, Thése de doctorat, INP-Toulouse, France, 1993.
[27] W.R.A. Goossens, G.L. Dumont, G.L. Spaepen, Chem. Eng. Prog. Symp. Ser. 67(116) (1971) 38–45.
[28] M. Sciazno, J. Bandrowski, L. Saroff, Inz. Chem. I. Proc. 10(3) (1985) 531–538.
[29] A.W. Nienow, P.N. Rowe, L. Cheung, Powder Technol. 20 (1978) 89–97.
[30] S. Chiba, T. Chiba, A.W. Nienow, H. Koyabashi, Powder Technol. 22 (1979) 255–269.
[31] N.S. Naimer, T. Chiba, A.W. Nienow, Chem. Eng. Sci. 37(7) (1982) 1047–1057.
[32] A. Kumar, P. Gupta, Ind. J. Technol. 12(5) (1974) 225–229.
[33] R.W. Rice, J.F. Brainovich, AIChE J. 32(1) (1986) 7–16.
[34] J.P. Peeler, J.R. Huang, Chem. Eng. Sci. 44(5) (1989) 1113–1119.
[35] A.W. Nienow, N.S. Naimer, T. Chiba, Chem. Eng. Commun. 62 (1987) 53–66.
[36] J.F. Richardson, Incipient fluidization and particulate system, in: J.F. Davidson, D. Harrison (Eds.), Fluidization, Academic Press, London, 1971.
[37] V. Thonglimp, Thèse de doctorat, INP-Toulouse, France, 1981.
[38] F. Zarza-Baleato, Thèse de doctorat, INP-Toulouse, France, 1986.
[39] J.V. Fletcher, M.D. Deo, F.V. Hanson, Powder Technol. 76 (1993) 141–147.
[40] S. Zerguerras, Thèse de doctorat, Université de Perpignan, France, 1996.
[41] G. Rovero, C.M.H. Brereton, N. Epstein, J.C. Grace, L. Casalegno, N. Piccinini, Can. J. Chem. Eng. 61(6) (1983) 289–296.
[42] H. Tho-Ching, N. Yutani, L.T. Fan, W.P. Walawender, Powder Technol. 35 (1983) 249–257.
[43] J. Adanez, J.C. Abanades, Powder Techol. 67 (1991) 113–119.
[44] H. Toyohara, Y. Kawamura, Int. Chem. Eng. 32(1) (1992) 164–171.
[45] P. Bourgeois, P. Grenier, Can. J. Chem. Eng. 46 (1968) 325.
[46] S. Saxnena, G. Vogel, Trans. Int. Chem. 55 (1977) 184–189.
[47] J.F. Richardson, M.A. St Geronimo, Chem. Eng. Sci. 34 (1979) 1419–1427, quoted in [26].
[48] V. Thonglimp, N. Hiquily, C. Laguerie, Powder Technol. 38 (1984) 233–253.
[49] V. Thonglimp, N. Hiquily, C. Laguerie, Powder Technol. 39 (1984) 223–239.
[50] A. Lucas, J. Arnaldos, J. Casal, L. Puigjaner, Ind. Eng. Chem. Process. Des. Dev. 25 (1986) 426–429.
[51] A. Barbosa, D. Steinmetz, H. Angelino, Fluidization VIII, Tours-France, vol. 1, Laguérie and Large, 1995, pp. 145–153.
[52] J. Talukdar, V. Mathur, AIChE Symp. Ser. Fluidization and Fluid Particle Systems 92(313) (1996) 36–39.
[53] F. Marble, The Phys. of Fluids 7(8) (1964) 1270–1282.